Intermediate Filaments in Non-Neuronal Cells of Invertebrates: Isolation and Biochemical Characterization of Intermediate Filaments from the Esophageal Epithelium of the Mollusc *Helix pomatia*

ECKART BARTNIK, MARY OSBORN, and KLAUS WEBER
Max Planck Institute for Biophysical Chemistry, D-3400 Goettingen, Federal Republic of Germany

ABSTRACT To screen invertebrate tissues for the possible expression of intermediate filaments (IFs), immunofluorescence microscopy with the monoclonal antibody anti-IFA known to detect all mammalian IF proteins was used (Pruss, R. M., R. Mirsky, M. C. Raff, R. Thorpe, A. J. Dowding, and B. H. Anderton. 1981. *Cell*, 27:419–428). In a limited survey, the lower chordate *Branchiostoma* as well as the invertebrates *Arenicola*, *Lumbricus*, *Ascaris*, and *Helix pomatia* revealed a positive reaction primarily on epithelia and on nerves, whereas certain other invertebrates appeared negative. To assess the nature of the positive reaction, *Helix pomatia* was used since a variety of epithelia was strongly stained by anti-IFA. Fixation–extraction procedures were developed that preserve in electron micrographs of esophagus impressive arrays of IFs as tonofilament bundles. Fractionation procedures performed on single cell preparations document large meshworks of long and curvilinear IF by negative stain. These structures can be purified. One- and two-dimensional gels show three components, all of which are recognized by anti-IFA in immunoblotting: 66 kD/pI 6.35, 53 kD/pI 6.05, and 52 kD/pI 5.95. The molar ratio between the larger and more basic polypeptide and the sum of the two more acidic forms is close to 1. After solubilization in 8.5 M urea, in vitro filament reconstitution is induced when urea is removed by dialysis against 2–50 mM Tris buffer at pH 7.8. The reconstituted filaments contain all three polypeptides. The results establish firmly the existence of invertebrate IFs outside neurones and demonstrate that the esophagus of *Helix pomatia* displays IFs which in line with the epithelial morphology of the tissue could be related to keratin IF of vertebrates.

Whereas actin(s) and tubulin(s) seem established as general cytoplasmic components of most if not all eucaryotic cells, knowledge of intermediate filament (IF)[1] proteins and their characterization is restricted in large part to vertebrates and here particularly to mammals. Extensive studies on warm-blooded vertebrates have demonstrated the cell- and tissue-specific expression patterns of the five subclasses of IF proteins that parallel known rules of embryonic differentiation (14, 23, 33, 41). Due to their usefulness in cell and tumor typing, much of IF research has subsequently centered around human cells. However, since the function(s) of IFs is still open to debate, one possible approach to function is to ask how widespread IFs are throughout the animal kingdom. Although it is clear from biochemical, immunological, and cell morphological data that IFs exist in cold-blooded vertebrates (see for instance references 11, 16, and 46), even in these phyla the rules of cell type–specific expression patterns are largely undocumented. Evidence for IFs in invertebrates is not only extremely sparse but often very confusing. Although the presence of neurofilaments is firmly established by morphological and biochemical criteria for the annelid *Myxicola* (8, 20, 31, 43) and the molluscs *Loligo* (31, 43, 54) and *Aplysia* (32),

[1] *Abbreviations used in this paper:* IF, intermediate filament; PMSF, phenylmethylsulfonyl fluoride; TAME, *n*-tosyl-L-arginine methyl ester.

there are repeated claims from electron microscopic data that arthropods lack neurofilaments (3, 35; see also references 32 and 51). Nevertheless, *Drosophila* cells in culture reveal a 46-kD protein that could be an IF protein as it seems to be recognized by a monoclonal antibody known to detect all mammalian IF proteins and also shows immunological cross-reactivity with vertebrate vimentin as seen with a further monoclonal antibody (9, 51). However, recent hybridization studies with cDNA probes for mammalian vimentin and desmin have not detected corresponding genes in *Drosophila* (46), and the same negative result is obtained with probes covering the human epithelial keratins (16). As morphological evidence for IF in *Drosophila* cells is rather poor, one is left with only the firmly established neurofilaments in *Myxicola*, *Loligo*, and *Aplysia*, as well as the occasional ultrastructural report on the possibility of IFs in some non-neuronal tissues such as the tube foot of the echinoderm *Strongylocentrotus purpuratus* (22) and certain cells of the leech (45), *Aplysia* (5), and the earthworm (26; see also reference 2), which display fibrils connected to plaque-bearing membrane domains resembling desmosomes of vertebrates. Since in the latter cases no biochemical evidence is available, the question of IF outside neurones remains open for invertebrates.

As an independent approach towards characterizing invertebrate IF proteins, we have used the mouse monoclonal antibody anti-IFA isolated by Pruss et al. since it seems to recognize many if not all mammalian IF proteins (44), and its epitope has been located to the carboxyterminal end of the structurally conserved coiled–coil domain seen so far in all IF proteins (18, 52). Although this antibody recognizes different human keratins with rather different affinities (6), its epitope location to a particularly highly conserved part of mammalian IF proteins as well as its demonstrated reactivity with *Myxicola* neurofilaments (44) seemed properties that might be useful in exploring IF expression in invertebrates. Here we report anti-IFA staining on tissue sections of certain invertebrate species. After this preliminary survey, we have characterized the IF display in the mollusc *Helix pomatia* by several techniques. Improved fixation procedures have allowed the electron microscopic documentation of striking tonofilament-like IF bundles and the parallel display of anti-IFA immunoreactive material with morphologically distinct IFs. Such material when purified from *Helix* esophagus displays properties reminiscent of those of vertebrate keratin proteins.

MATERIALS AND METHODS

Animal Species: *Helix pomatia*, the vinyard snail, and *Lumbricus terrestris* were collected near Bonn and Goettingen. Animals were kept at 8°C in a terrarium. *Ascaris lumbricoides suum* was taken from pig intestine at the local slaughterhouse. The following marine invertebrates were purchased from the Biologische Anstalt (Helgoland, FRG): *Actinia equina, Arenicola marina, Asterias rubens, Cancer pagurus, Ciona intestinalis, Crangon crangon*, and *Psammechinus miliaris*. The chordate *Branchiostoma lanceolatum* was from the same source. Tissues were isolated by dissection.

Antibodies: The hybridoma clone anti-IFA (44) was a gift from Dr. Martin Raff and is also available from the American Type Culture Collection, Rockville, MD (ATCC No. TIB131). Since the anti-IFA clone was isolated from a fusion of C3H/He mouse spleen cells and the cell line NS-1 (a BALB/c derivative), ascites fluid was produced in athymic immunodeficient mice (C3/Hehan nu/nu) (Zentralinstitut für Versuchstiere, Hannover, FRG). In the current experiments, ascites fluid was usually diluted 1:40, which corresponded to ~100–170 μg mouse IgG/ml as estimated by an ELISA test. The monoclonal tubulin antibody YL 1/2 (27) was a gift from Drs. J. Kilmartin and J. Wehland. Nitrobenzoxadiazole-phallicidin was purchased from Molecular Probes (Junction City, Oregon) and used at a final concentration of 0.16 μg/ml.

Immunofluorescence Microscopy on Frozen Tissue Sections: Small fragments of tissue were snap-frozen in isopentane cooled with liquid nitrogen to −140°C. 4–5-μm-thick sections were cut on a cryostat. Air-dried sections were fixed with 95% ethanol/5% acetic acid for 8 min at −10°C. After rehydration in phosphate-buffered saline (PBS) and several washes, sections were exposed for 1 h at 37°C to anti-IFA. Sections were then washed with PBS and further incubated with rhodamine-labeled goat anti–mouse antibodies (Cappell Laboratories, Cochranville, PA) diluted 1:20 in PBS. After further washes, samples were mounted in Mowiol 4–88. For a review of snail anatomy see references 29 and 47.

Immunofluorescence Microscopy on Single Cell Preparations: *Helix* esophagus was cut into 2–3-mm broad rings that were turned inside-out by forcing them over 5-mm-thick glass rods. The tissue was fixed first for 2 min at 20°C with 2% formaldehyde in PBS, washed in PBS, and then extracted twice for 10 min at 20°C with 50 mM PIPES pH 6.8 containing 50 mM NaCl, 0.5% Triton X-100, 1 mM EGTA, 1 mM EDTA, and 0.1 mM phenylmethylsulfonyl fluoride (PMSF) containing also the protease inhibitors *n*-tosyl-L-lysine chloromethyl ketone and *n*-tosyl-L-arginine methyl ester (TAME) at 0.1 mM. After a wash in PBS containing 1 mM EDTA and 1 mM EGTA, the tissue rings were cut open, removed from the glass rods, and placed on a glass slide. Epithelial cells were gently removed by scraping the top of the specimen with a coverslip and were resuspended in PBS containing 1 mM EDTA and 1 mM EGTA. The cell suspension was passed several times through a 5-ml syringe with a 0.9 × 40-mm needle to provide a preparation consisting in large part of single cells (4, 12). These were allowed to settle onto polylysine-coated glass coverslips. A brief centrifugation in a clinical centrifuge (5 min, 4,000 rpm) increased the number of single cells adhering to the glass. After a brief wash with PBS, cells were processed for immunofluorescence microscopy by adding anti-IFA.

Electron Microscopy and Immunoelectron Microscopy on Single Cell Preparations: In our first experiments (e.g., Fig. 3, *A* and *B*), invertebrate tissues were subjected to electron microscopy using conventional fixation procedures suitable for vertebrate cells and tissues. Material was fixed in 2% glutaraldehyde in 0.109 M sodium cacodylate (pH 7.2), 0.109 M sucrose for 45 min at 20°C. After washing three times for 10 min at 20°C in 0.1 M cacodylate (pH 7.2), 0.1 M sucrose, cells were fixed with 2% osmium tetroxide in the same buffer for 30 min on ice. Cells were washed three times for 5 min at 4°C using 0.1 M cacodylate, 0.1 M sucrose. After washing for 5 min at 4°C in water, material was stained with 1% uranylacetate, dehydrated through an alcohol series, and embedded in Epon. Sections were contrasted with uranyl acetate and lead citrate.

In later experiments (e.g., Fig. 4, *D* and *E*, and Fig. 5), single cell preparations prepared exactly as above for immunofluorescence microscopy were treated first with anti-IFA and then with gold-labeled goat anti–mouse antibodies G10 (10-nm gold; Janssen Pharmaceutica, Beerse, Belgium). They were then fixed in the glutaraldehyde-cacodylate buffer given above, and processed as described except that the specimens were flat embedded in Epon.

Negative Staining of Triton X-100–extracted Esophageal Cells: Single cells that had not been fixed with formaldehyde were extracted using the Triton buffer given above for the immunofluorescence microscopy procedure. The resulting suspension was pelleted and resuspended in PBS. A drop put on a microscope slide was covered with a carbon film. The slide was inverted to allow material to attach to the film, which was subsequently taken up with a 400-mesh copper grid. After staining with 2% uranyl acetate, the preparation was examined by electron microscopy.

Purification of IF From Helix Esophagus: Tissue was excised, rinsed with PBS, and cut lengthwise. Epithelial cells were gently scraped off using a coverslip. Cells were washed in PBS containing EDTA and EGTA at 1 mM. Single cell preparations were obtained by passing the suspension through a syringe (see above). Cells were harvested in an Eppendorf bench top centrifuge. 0.1 g of finely minced tissue or the esophagal cell pellet were homogenized by 10 strokes of a glass-teflon potter homogenizer in 1.6 ml of extraction buffer: 50 mM PIPES pH 6.9, 100 mM NaCl, 300 mM sucrose, 2 mM $MgCl_2$, 3 mM KCl, 10 mM EGTA, 0.5% Triton X-100. After 5 min on ice, the sample was centrifuged for 10 min at full speed in an Eppendorf centrifuge. The resulting pellet was extracted twice more as described. The final pellet was resuspended in 1.6 ml 50 mM PIPES pH 6.9, 50 mM NaCl, 300 mM sucrose, 3 mM $MgCl_2$ containing pancreatic RNAse (Merck, Darmstadt, FRG) and DNAse (Miles Scientific, Munich, FRG), both at 100 μg/ml. After incubation for 15 min at 20°C, centrifugation was done as above. The pellet was resuspended in 1.6 ml of 10 mM Tris-HCl pH 7.4, 140 mM NaCl, 2 mM MgCl, 10 mM EGTA and again centrifuged. All buffers were 0.1 mM in the protease inhibitors PMSF, *n*-tosyl-L-lysine chloromethyl ketone, and TAME.

IF Reassembly In Vitro: The final pellet (see purification of IF from

Helix esophagus) was dissolved in 8.5 M urea, 20 mM Tris-HCl (pH 8.0) containing 30 mM 2-mercaptoethanol and 0.1 mM PMSF. The solution was made 1 mg/ml in protein and centrifuged 10 min at 10,000 *g* and then 90 min at high speed, providing a clear supernatant that was frozen in aliquots. These were dialyzed at 4°C against different assembly buffers. In the first set of experiments, dialysis was against 1 mM Tris-HCl (pH 8) containing 10 mM 2-mercaptoethanol and 0.1 mM PMSF. The quality of the reassembled filaments was further improved by a three step procedure previously used for mammalian keratins (25). Aliquots of 0.25 mg/ml protein were dialyzed from 8.5 M urea for 3 h against 4 M urea, 2 mM Tris-HCl (pH 8), 25 mM 2-mercaptoethanol, then for 12 h against 10 mM Tris-HCl (pH 7.8), 25 mM 2-mercaptoethanol, and finally for 3 h against 50 mM Tris-HCl (pH 7.8), 25 mM 2-mercaptoethanol. All solutions contained PMSF at 0.01 mM. The sample of assembled filaments shown in Fig. 6*B* was obtained by the three step procedure. For negative staining, a carbon film was put on a drop of the filament solution. The film was taken up with a 400-mesh copper grid and stained with 2% uranyl acetate.

Gel Electrophoresis and Immunoblots: One-dimensional gel electrophoresis was according to Laemmli (30) using slab gels with 10 or 12.5% acrylamide (0.5 × 75 × 100 mm). Marker proteins were human spectrin, rabbit phosphorylase b, bovine serum albumin (BSA), porcine vimentin, bovine muscle actin, and bovine chymotrypsinogen. Two-dimensional gels were according to O'Farrell (39). Pellets were solubilized in 10 mM Na-K-phosphate buffer, 5% SDS, and 10% 2-mercaptoethanol. Proteins recovered by acetone precipitation were dried under nitrogen. Aliquots were dissolved in the lysis buffer given by O'Farrell. Isoelectric focusing in the first direction was in capillary tubes (36) with an inner diameter of 1.5 mm and a length of 92 mm. Ampholines covering the range 3.5–10 were from LKB (Bromma, Sweden). The second direction was on 10% slab gels (0.5 × 75 × 100 mm). Marker proteins were used for both directions. For the first dimension, BSA, porcine vimentin, bovine skeletal muscle actin, and yeast 3-phosphoglycerate kinase were used. Isoelectric points were evaluated from parallel capillary gels by extracting gel slices and measuring the pH. Our gel coordinates differ slightly from those given by Moll et al. (34). Their values for BSA, rabbit muscle actin, and human vimentin are 6.4, 5.4, and 5.2, respectively. Our values for BSA, bovine muscle actin, and porcine vimentin are 6.2, 5.7, and 5.5, respectively. The isoelectric points given for *Helix* proteins were calculated from our coordinates using the most basic isoform of each species. Thus, the highest molecular weight species with an apparent pI of 6.35 is slightly more basic than is BSA, to which we assigned a pI of 6.2.

One- and two-dimensional gels were used for the electrophoretic protein transfer to nitrocellulose (49). Quality of transfer was monitored by staining with Ponceau red. Immunoblots were reacted with anti-IFA at 60 μg/ml for 2 h at 37°C followed by peroxidase-labeled rabbit anti-mouse antibodies (Boehringer Ingelheim, FRG) diluted 1:200 for the same time.

RESULTS

Immunofluorescence Microscopy on Invertebrate Tissues

Figs. 1 and 2 provide staining patterns obtained on frozen tissue sections from different species in indirect immunofluorescence microscopy using the mouse monoclonal antibody anti-IFA. The data are summarized in Table I. Fixation was in all cases with 95% ethanol/5% acetic acid, since IFA hybridoma supernatant fractions stained IFs in cultured mammalian cells in our hands reliably only after this fixation procedure and not after the more usual cold methanol or acetone fixation procedures.

Fig. 1 gives a survey of anti-IFA on various vertebrate and invertebrate tissues using a constant dilution of anti-IFA ascites fluid (~130 μg mouse IgG/ml). Fig. 1, *A* and *B* shows staining of human and rat intestine. In both instances, the epithelial cells as well as some other cell types were strongly positive in immunofluorescence. A brief survey of other tissues from human and rat showed strong staining of cells such as fibroblasts and chondrocytes, of vascular and visceral smooth muscle cells, and although less strongly, of Z-lines in skeletal muscle. Positive staining was also seen in the chordate *Branchiostoma* in which the one-layered epidermis as well as some nervous tissue showed strong decoration (Fig. 1, *C* and *D*; for previous ultrastructural evidence of tonofilaments in the epidermis of lower chordates, see for instance reference 40). In the annelid *Arenicola*, intestinal epithelium as well as other cell types were strongly positive (Fig. 1*F*), and in *Lumbricus*, anti-IFA stained intestinal epithelium (Fig. 1*E*) as well as epidermis and muscle. In the nematode *Ascaris*, strong staining was seen in the syncytial epidermis as well as in muscle cells (Fig. 1*G*). In *Helix pomatia*, a variety of different epithelia as well as nerves were strongly stained with anti-IFA (Fig. 1*H*; Fig. 2, *A–H*). The striking fact about the sections from invertebrate tissue shown in Fig. 1 is the strong

TABLE I. *Decoration of Tissues from Various Invertebrate Species with the Antibody Anti-IFA*

Phylum	Species	Epithelia	Nerve tissue
Chordata	*Branchiostoma*	Epidermis	Cells within muscle and spinal cord
Echinodermata	*Asterias*	—	—
	Psammechinus	—	—
Arthropoda	*Cancer*	—	—
	Crangon	—	—
	Drosophila	—	—
Annelida	*Lumbricus*	Epidermis Intestinal epithelium	Ventral giant Nerve fibers
	Arenicola	Epidermis Intestinal epithelium	
Nemathelminthes	*Ascaris*	Syncytial epidermis	Nerve cord
Mollusca	*Helix*	Epidermis Internal epithelium of esophagus, stomach, intestine, lung, kidney	Tentacle nerves Ganglia
Cnidaria	*Actinia*	—	—
Ciliata	*Tetrahymena*	—	—

Tissues noted are those in which positive staining was seen with anti-IFA. —, no staining observed under the conditions of this survey. Tissues were dissected and immediately snap-frozen. 4–5-μm thick sections were cut on a cryostat, air-dried, and fixed with 95% ethanol/5% acetic acid for 8 min at −10°C. PBS-rehydrated sections were exposed for 1 h at 37°C to anti-IFA, washed, and labeled with rhodamine-labeled goat anti-mouse antibodies. The results of this table come from a preliminary survey made under the conditions specified above. Invertebrate species that showed no staining of either epithelia or of neuronal tissue also showed no staining of muscle and connective tissue present in the same sections. In two species, *Lumbricus* and *Ascaris*, both muscle cells and cells of the connective tissue appear to be positive with anti-IFA (Fig. 1).

decoration of epithelial cells. Nervous tissue is also stained in the instances shown. In several species such as the chordate *Branchiostoma* and also the invertebrate *Helix*, muscle cells and cells of the connective tissue, which at least in warm-blooded vertebrates are known to contain IFs remained unstained. Table I shows that a preliminary survey of other invertebrates, and in particular *Asterias*, *Psammechinus*, *Cancer*, *Crangon*, and *Drosophila*, revealed no positive staining with anti-IFA. In addition, no staining was observed in preliminary experiments on *Actinia* and *Tetrahymena*, which were selected as prototypes for the metazoa and the protozoa, respectively.

Immunofluorescence Microscopy of Helix pomatia Tissues

The results given in Fig. 1 raise the question of whether the positive reaction seen with anti-IFA did indeed indicate the presence of IFs. We concentrated further experiments on *Helix pomatia*, as it can be obtained locally, and different tissues can be prepared by dissection.

Fig. 2 shows immunofluorescence microscopy with anti-IFA on different tissues from *Helix pomatia*. The hematoxylin-eosin stain in Fig. 2*A* emphasizes that as in many other invertebrates, the epidermis is a simple epithelium consisting of a single cell sheet. A comparison of Fig. 2*A* with the immunofluorescence picture given at the same magnification in Fig. 2*B* shows that the epithelial cells of the foot are strongly positive with anti-IFA. At higher magnification, already some fibrillar structures are discerned (Fig. 2*C*). Internal epithelia of *Helix pomatia* were also strongly stained by anti-IFA. Thus, stomach (Fig. 2*D*), lung (Fig. 2*E*), intestine (not shown), and esophagus (see below and Fig. 1*H*) were strongly decorated. Neuronal staining was seen in the anterior pedal retractor muscle (Fig. 2*F*), in the cerebral ganglion (Fig. 2*G*), and in the eye tentacle (Fig. 2*H*). In the composite micrograph of the eye tentacle in Fig. 2*H*, staining of the epidermis can be visualized at the bottom and in a cross-section of the tentacle nerves at the top. In the *Helix* tissues examined, positive staining with anti-IFA was not seen on tissues other than epithelia and nerves. Thus, muscle tissues and in particular the pronounced foot muscle were not stained.

Titration of anti-IFA on *Helix* esophagus and epidermis showed a positive reaction in the concentration range of 10–130 μg/ml. In contrast, a variety of other polyclonal and monoclonal antibodies specific for keratin IF proteins in mammals were also screened on *Helix* foot epidermis. No reaction was seen with AE1, AE3 (6), K_G8.13.2 (19), or CK4 (7), used as hybridoma supernatants, or with a variety of polyclonal antibodies raised against either cow snout keratins or human foot epidermal keratins.

The immunofluorescence results using anti-IFA suggested that *Helix* esophageal epithelium might be a good source from which to further characterize invertebrate non-neuronal IFs. It is relatively easy to scrape the epithelial cells from the esophagus (see Materials and Methods), and by using several animals, sufficient material for biochemical experiments can be obtained.

Electron Microscopy on Epithelia From Helix pomatia

Initial attempts using head epidermis and esophageal tissue processed through standard electron microscopic procedures provided pictures such as those shown in Fig. 3, *A* and *B*. Although similar protocols used on vertebrate material result in clear documentation of IFs, the sections on invertebrate tissue revealed a very dense cytoplasm with little filamentous detail but well-preserved membraneous structures. Encouraged by the occasional but poorly documented filament bundle in these preparations (e.g., arrowheads in Fig. 3*A*), we developed a procedure to obtain single cells of esophageal epithelium and tried to optimize the conditions for IF preservation by parallel immunofluorescence microscopy. The final protocol found to be suitable for preserving IFs involved fixing the esophagus briefly with formaldehyde (2% for 2 min at 20°C) before extracting it with 0.5% Triton X-100 in the presence of a normal salt concentration. This procedure is given in detail in the Materials and Methods section. Epithelial cells were then removed by scraping, and several passages through a syringe provided a preparation of slightly extracted single cells or small islands of cells. When such material was directly exposed to anti-IFA followed by fluorescently labeled second antibody, a strong decoration of IFs was seen (Fig. 4*A*). These specimens revealed clearly pronounced bundles of filaments and showed an overall display rather similar to that seen in mammalian intestinal epithelium processed with keratin antibodies (e.g., references 12 and 13). The anti-IFA stain was not present in the microvilli zone at the apical side of the esophageal cells. Parallel stains with a fluorescently labeled phalloidin derivative documented the wealth of F-actin in the microvilli and the terminal web (Fig. 4*C*). Comparison of micrographs such as those shown in Fig. 4, *A* and *C* indicates that the putative intermediate filaments revealed by anti-IFA, though entering the terminal web, did not penetrate further into the apical zone. Some esophageal cells are ciliated, and this is demonstrated in Fig. 4*B* by staining with the tubulin monoclonal antibody YL 1/2 and parallel electron micrographs (not shown).

Electron microscopy performed on single esophagus cells of *Helix*, which had been briefly fixed with formaldehyde before Triton extraction, revealed impressive filament bundles

FIGURE 1 Staining patterns obtained with anti-IFA on different vertebrate and invertebrate tissues. Frozen sections were fixed in 95% ethanol/5% acetic acid and incubated with anti-IFA monoclonal antibody followed by rhodamine-labeled goat anti-mouse IgGs. Anti-IFA recognizes epithelial cells in both human (*A*) and rat (*B*) intestine (some staining of connective and smooth muscle tissue is seen particularly in *B*). In the chordate *Branchiostoma* (*C* and *D*), the single cell-layered epidermis (*e*) as well as some nerve cells within the muscle (arrowhead in *C*) and the spinal cord (*D*) are positively labeled by anti-IFA. The annelids *Lumbrius* (*E*) and *Arenicola* (*F*) show staining by anti-IFA of the epidermis (*e*) as well as of some connective tissue cells, and of circular and longitudinal muscles (*m*; all in *E*), as well as of the intestinal epithelium where bundles of filaments can be clearly distinguished in the epithelial cells (*F*). In the nematode *Ascaris*, the syncytial epidermis (*e*) as well as muscle cells (*m*) are stained by anti-IFA (*G*). The cuticle (*c*) is negative. In *Helix*, the esophageal epithelium is strongly stained by anti-IFA (*H*) *A–E*, *G*, and *H*, × 160. *F*, × 640.

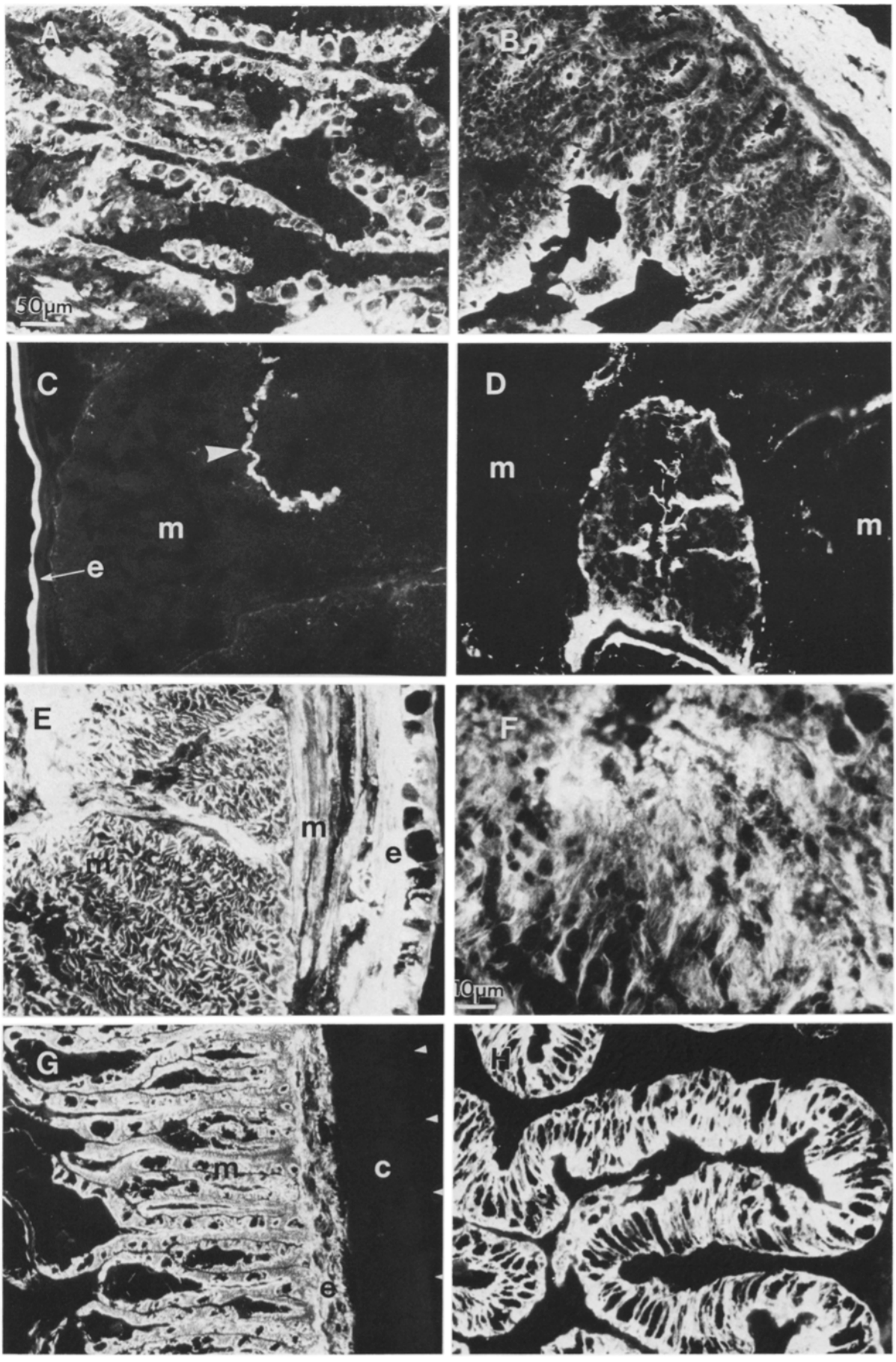
A
50μm
B
C
m
e
D
m
m
E
m
m
e
F
10μm
G
m
c
e
H

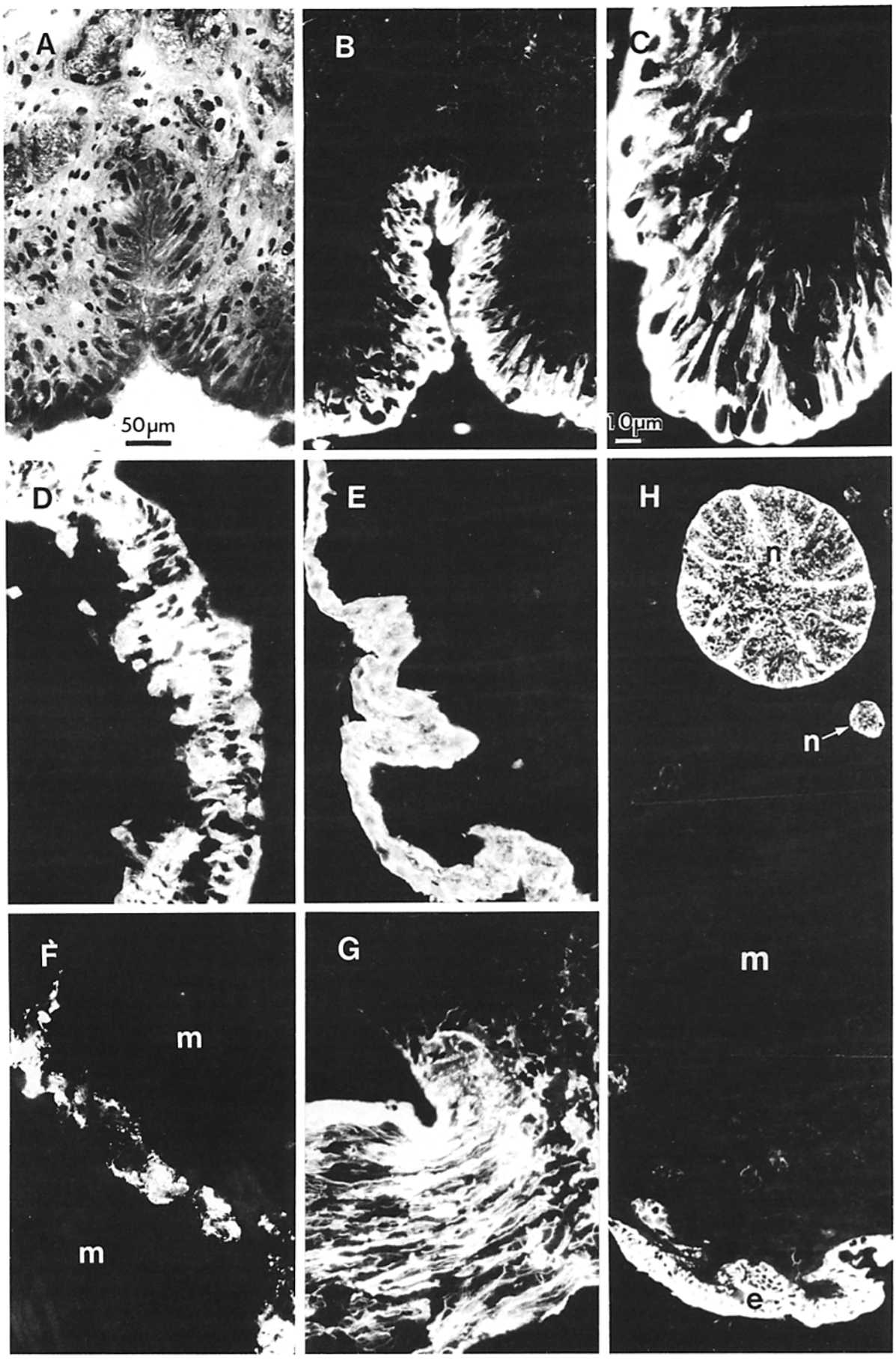
A
50μm
B
C
D
E
H
n
n
m
F
m
m
G
e

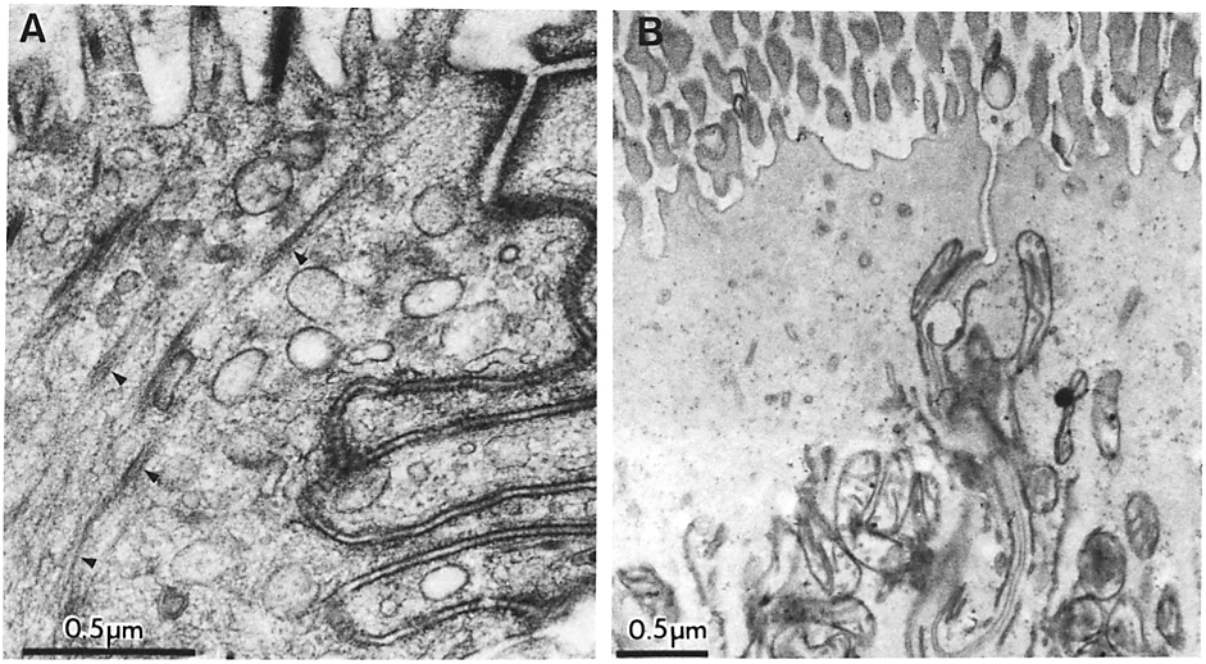

FIGURE 3 Electron microscopy of *Helix* tissues using conventional fixation procedures. (*A*) *Helix* mantle epidermis after fixation with 2% glutaraldehyde (see Materials and Methods). Arrowheads point to poorly preserved filamentous arrays lying between the basal part of the cell and the microvilli. (*B*) *Helix* esophagus. Fixation as in *A*. Filaments have not been preserved. *A* and *B* should be directly compared to Fig. 5. *A*, × 46,700. *B*, × 24,500.

from which occasional single filaments seemed to emanate (Fig. 5, *A–C*). Their often curved appearance and dense packing is reminiscent of the tonofilaments documented by many papers in a large variety of vertebrate epithelia known to have keratin IFs. Single filaments occurring in specimens such as those shown in Fig. 5 measure 7–8 nm in diameter. IFs are well preserved in these cytoskeletons, particularly when they occur in bundles. Microfilaments of the apical zone (microvilli and brush border) are, however, relatively poorly preserved.

The similarity between the fluorescent micrographs and the tonofilaments documented by electron microscopy invited the use of gold-labeled second antibodies. In these experiments, isolated esophagal cells were treated by the same methods used for immunofluorescence microscopy. However, instead of a fluorescently labeled antibody, a second antibody carrying 10-nm gold was used. Subsequent electron microscopy was performed as before. Fig. 4, *D* and *E* shows that specific but sparse labeling occurred both on tonofilament bundles and on single filaments. An internal control of the specificity of labeling is given by the virtual lack of label in the apical zone. Parallel samples treated with a mouse monoclonal antibody to mammalian vimentin followed by the gold-labeled second antibody showed no decoration.

Given the abundance of IFs present in electron micrographs of the esophagal cells, we examined extracted esophagus cells not previously fixed with formalin. Such material was extracted with Triton X-100, pelleted, and then diluted and negatively stained. As shown in Fig. 6*A*, a dense meshwork of long smooth and curvilinear filaments is observed. These measure ~7–8 nm in diameter and resemble in morphology mammalian IFs shown in numerous preparations from various laboratories.

Biochemical Characterization of Intermediate Filaments From Helix Esophagus

Extraction of esophagus cells was as in Materials and Methods. Lane *2* in Fig. 7*A* documents the polypeptides present in the total cell extract, and lane *3* shows the polypeptides left after Triton and moderate salt extraction in the final pellet. Three major polypeptides of 66, 53, and 52 kD are retained in the latter preparation (Fig. 7*A*, lane *3*). The two lower molecular weight species were sometimes poorly resolved from each other (see, for instance, Fig. 7*A* versus the gel in Fig. 7*C* at the right side). A minor band at the position of actin and two other bands of lower molecular weight are also seen. The relative abundance of these contaminants is variable in different preparations, and they are absent in reconstituted filaments (lane *5* of Fig. 7*A*; see below). Immunoblotting experiments show that all three major polypeptides react strongly with the anti-IFA antibody (see Fig. 7*B*, lane *1*). Three additional but very faint bands seen in the blot are virtually absent in the original sample stained with dye (Fig. 7*B*, lane *1*). The lower one could be a proteolytic degradation product, whereas the nature of the two faint bands situated

FIGURE 2 (*A*) Hematoxylin-eosin and (*B–H*) anti-IFA staining of various tissues from *Helix pomatia*. (*A* and *B*) low and (*C*) high power views of foot sole epidermis. (*D*) Stomach epithelium, (*E*) lung epithelium, (*F*) neuronal cells within the anterior pedal retractor muscle, (*G*) cerebral ganglia, and (*H*) cross-section of the eye tentacle. *e*, epidermis; *m*; muscle; *n*, tentacle nerves. Note that a variety of cells of epithelial and neural origin are positively stained by anti-IFA, and that filament bundles can already be recognized, for example in the section given in (*C*). *A*, *B*, and *D–H*, × 160. *C*, × 470.

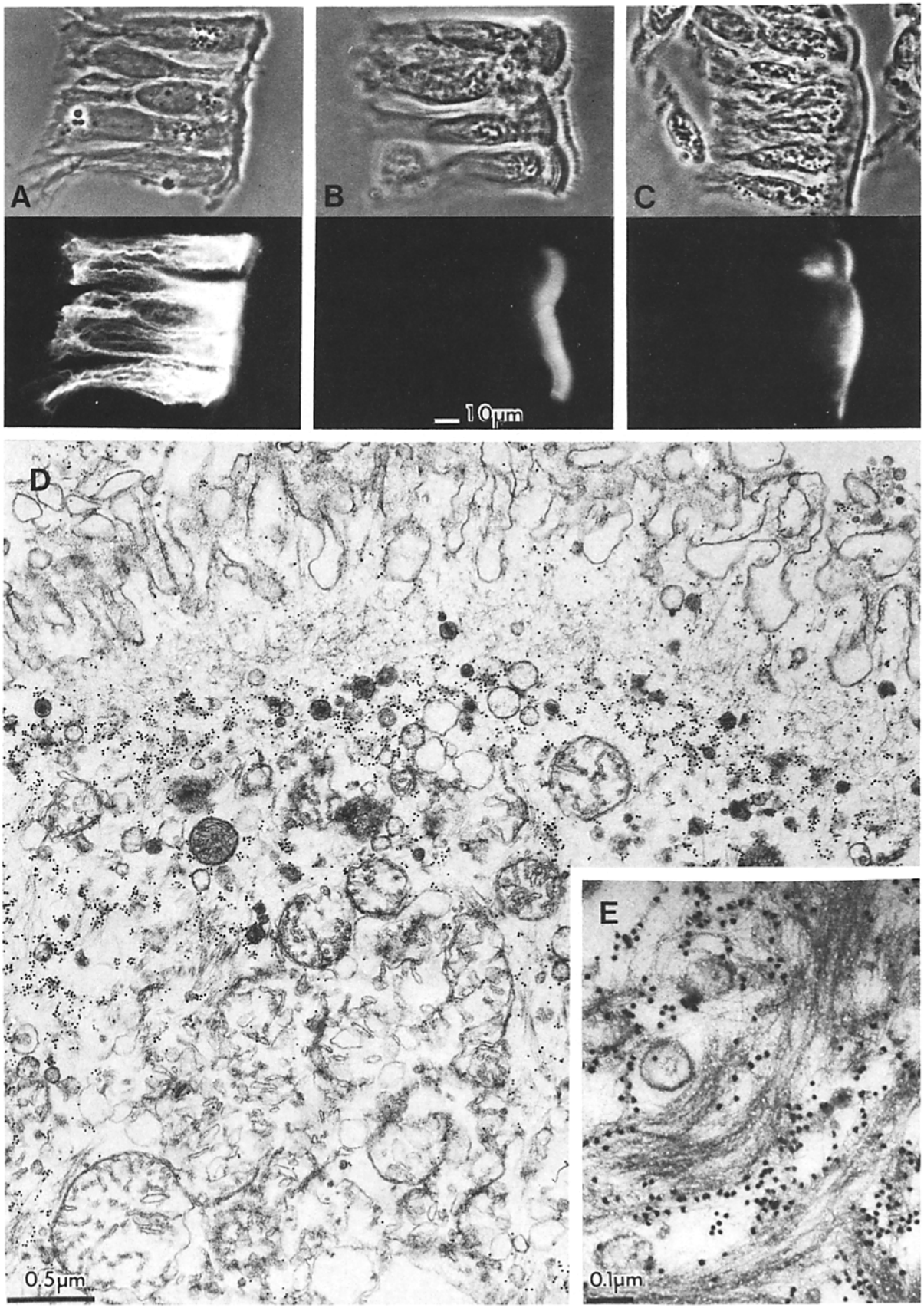

FIGURE 4 (*A–C*) Immunocytochemistry and (*D* and *E*) immunoelectron microscopy on isolated *Helix* esophageal cells with anti-IFA. Cells are stained either with anti-IFA to reveal the IF arrangement (*A*), with the monoclonal antibody YL 1/2 to reveal the arrangement of tubulin (*B*), or with nitrobenzoxadiazole-phallacidin to reveal the arrangement of actin (C). Most esophageal cells have microvilli (*A* and C) but some are in addition ciliated (*B*) (see also the corresponding phase contrast micrographs). (*D* and *E*) Cells fixed for 2 min in 2% formaldehyde, extracted with Triton, and processed for immunoelectron microscopy using anti-IFA as the first antibody and 10-nm gold-labeled goat anti-mouse IgGs as the second antibody. *A–C*, × 400. *D*, × 30,000. *E*, × 83,000.

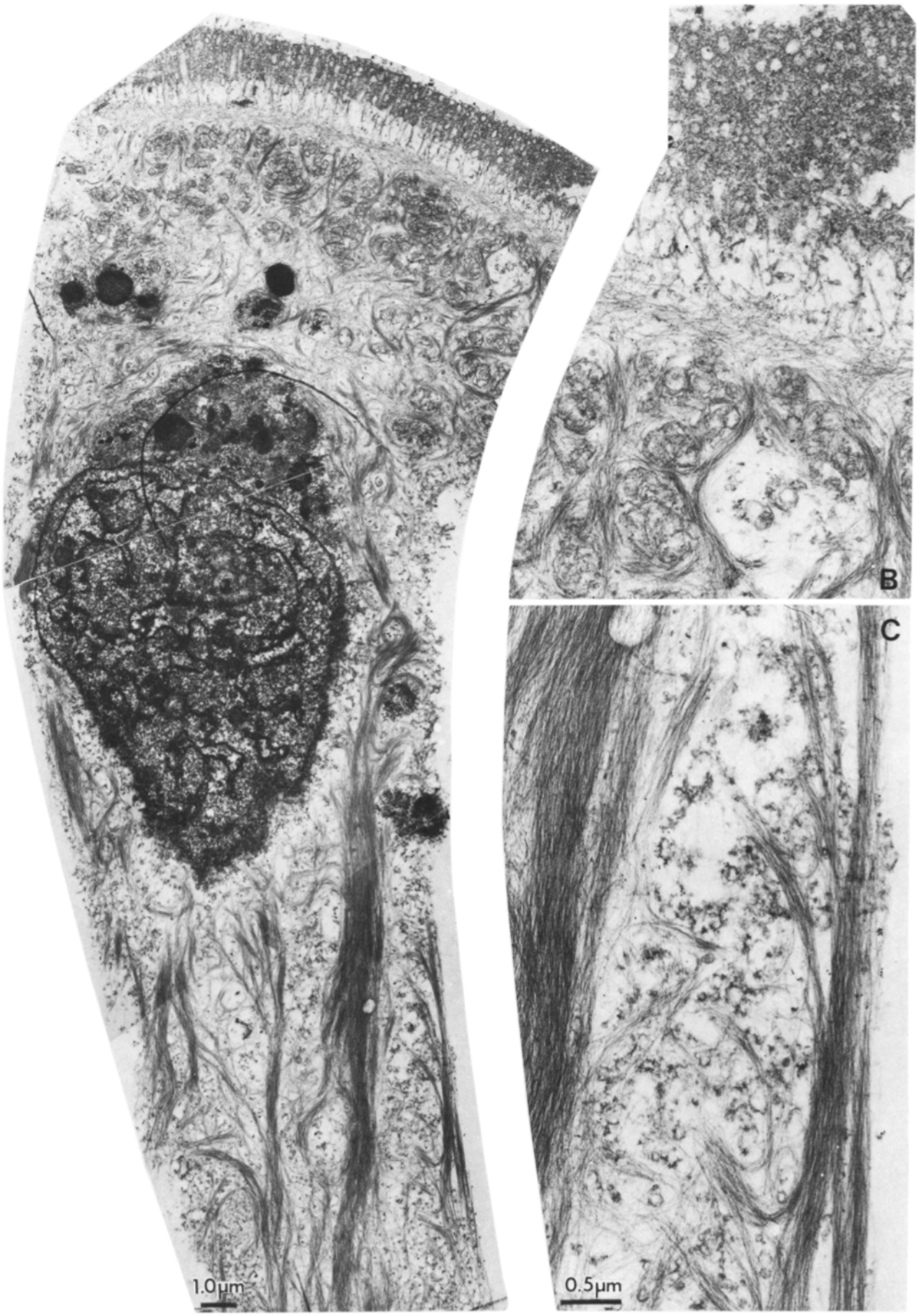

FIGURE 5 Electron microscopy of cells from *Helix* esophagus using the extraction and fixation procedures described in Materials and Methods. (*A*) Survey electron micrograph of isolated *Helix* esophageal cells. *B* and *C* show higher power views of parts of the same cell. Note that bundles of IFs (tonofilaments) as well as a single IF can be clearly visualized in *A–C*. Compare the preservation in these micrographs to that in Fig. 3, *A* and *B*. *A*, × 6,900. *B* and C, × 22,000.

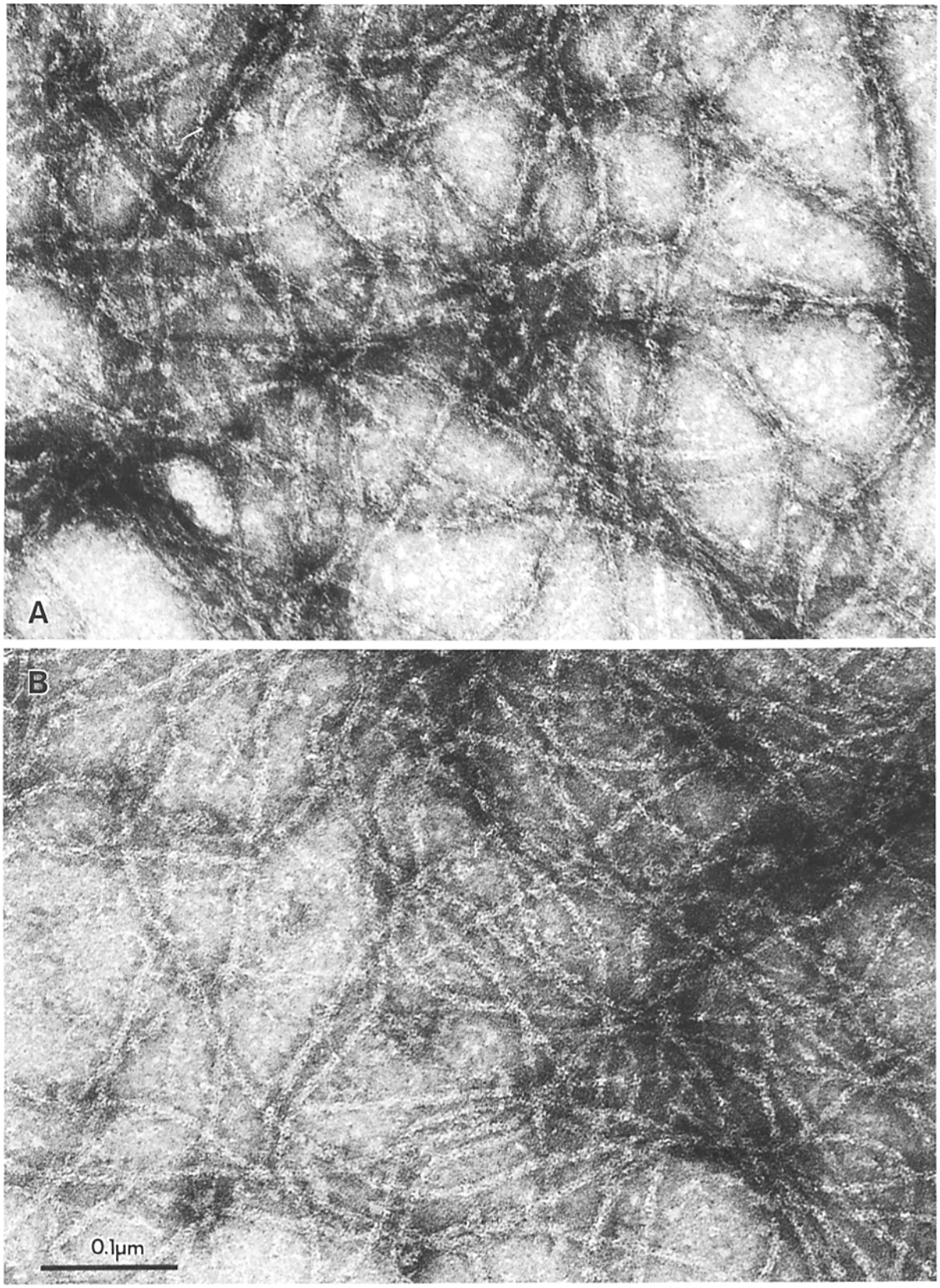

FIGURE 6 Electron microscopy of IFs from *Helix* by negative stain. (*A*) Stained preparations of IFs found in extracted *Helix* esophageal cells after dilution (see text). (*B*) Negatively stained filaments reassembled in vitro from urea-solubilized *Helix* IF proteins. Filaments have a diameter of 7–8 nm in both micrographs. *A* and *B*, × 235,000.

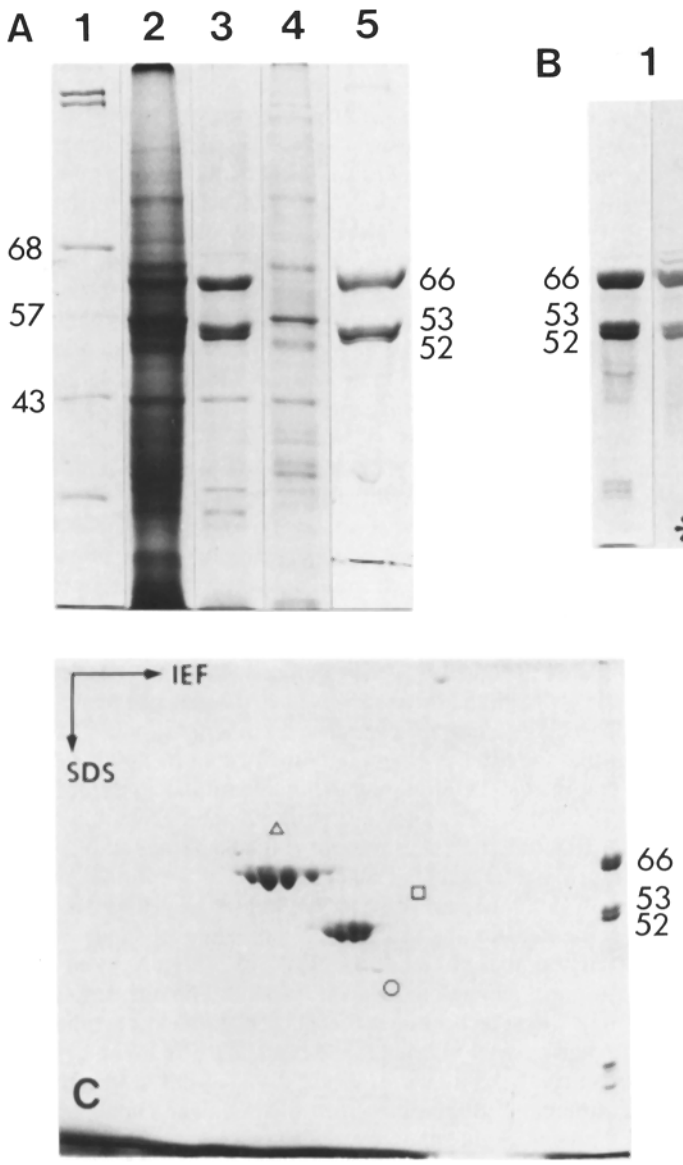

FIGURE 7 One- and two-dimensional gel electrophoresis of preparations from *Helix* esophagus enriched in IFs. (*A*) Lane *1*, marker proteins including human spectrin (doublet close to top), BSA (68 kD), porcine vimentin (57 kD), porcine muscle actin (43 kD), and chymotrypsinogen; lane *2*, *Helix* esophagus total cell extract; lane *3*, final pellet fraction of purified IF; lane *4*, supernatant after extraction with NaCl and Triton; lane *5*, pellet of in vitro reconstituted IFs. Note the prominent bands visible at 52, 53, and 66 kD in lanes *3* and *5*. (*B*) Coomassie Blue stain and corresponding immunoblots (designated by asterisks) of pellets after Triton extraction of various tissues. Lane *1*, *Helix* esophagus; lane *2*, *Helix* foot muscle; lane *3*, *Actinia toto* (whole animal). (C) Two-dimensional Coomassie Blue–stained gel of *Helix* esophagus IFs. △, BSA; □, porcine vimentin; ○, bovine muscle actin. IEF and SDS indicate the directions of isoelectric focusing (first dimension) and sodium dodecylsulfate gel electrophoresis (second dimension). The separation of the two lower molecular weight IF proteins (53 and 52) is somewhat variable. Note the good separation in the one-dimensional lane of C (right) versus the poorer resolution in *A* and *B*.

above the 66-kD species is currently unknown. Similar preparations either from *Helix* muscle (Fig. 7*B*, lane *2*) or from whole *Actinia* (Fig. 7*B*, lane *3*) showed no reactivity in immunoblots, consistent with the results for these tissues obtained in immunofluorescence microscopy (see above).

Two-dimensional gels performed on isolated esophagus IFs were used to further characterize the three major components seen in one-dimensional gels. As shown in Fig. 7*C*, each of the three polypeptides separate into different isoelectric variants of constant molecular weight but different isoelectric points. As IF proteins and particularly keratins from mammals give different isoforms due to differing degrees of phosphorylation (see for instance reference 34), we have used the most basic form in providing gel coordinates. In addition, as have others (6, 34), we incorporated known marker proteins as internal standards. As shown in Fig. 7*C*, there is one more basic and larger component (66 kD/pI 6.35) versus two more acidic and smaller components (53 kD/pI 6.05 and 52 kD/pI 5.95). Gel scans from one-dimensional gels were used to calculate their relative abundance. Correcting for the different apparent molecular weights, the molar ratio between the 66 kD and the sum of 53 and 52 kD was 0.95. Currently, we do not know if the 52-kD protein is derived proteolytically from the 53-kD protein. We also note that occasionally the 66-kD protein occurs as a doublet.

In Vitro Reconstitution of Helix Esophageal Filaments

IFs purified from *Helix* esophagus were solubilized in 8.5 M urea, and different protocols were tried to obtain *in vitro* reconstitution of filaments. The reconstituted filaments shown in Fig. 6*B* were obtained by a three step dialysis procedure (cf. 25) using as a first step 4 M urea with virtually no salt and then raising the Tris buffer concentration stepwise from 10 to 50 mM. In the last two steps, we found that it was essential to keep the pH at or above 7.8 to prevent aggregation and subsequent precipitation. Our assembly conditions resulted in long and morphologically distinct 7–8-nm filaments resembling those of the starting material (compare parts *A* and *B* of Fig. 6). When such reconstituted filaments are harvested, subsequent gel electrophoresis showed the presence of all three major polypeptides (Fig. 7*A*, lane *5*) found in the original sample.

TABLE II. *Amino Acid Composition of IF Isolated from Helix Esophagus and Then Reconstituted In Vitro*

Amino acid	Composition
	mol %
Ala	9.1
Arg	7.1
Asp	9.6
Cys	n.d.
Glu	17.1
Gly	7.1
His	3.0
Ile	4.9
Leu	9.0
Lys	7.0
Met	1.2
Phe	2.0
Pro	2.8
Ser	8.1
Thr	5.1
Trp	n.d.
Tyr	3.1
Val	3.9

n.d., not determined. For purity of fraction see Fig. 7*A*, lane 5.

Amino acid analysis was performed on reconstituted IFs (Fig. 7*A*, lane 5). The results (Table II) emphasize a low content of proline versus high values of aspartic acid, alanine, leucine, lysine, arginine, and particularly glutamic acid. These results are in line with general observations made on various mammalian IF proteins that have conserved domains high in α-helical content and can form coiled-coils. We note, however, that the moderate glycine value (7%) is relatively higher than those values encountered in various nonepithelial IF proteins (see for instance reference 17). On the other hand, it is much lower than are the elevated values of glycine documented for various mammalian epidermal keratins (see for instance reference 15) whose high glycine content is due to very glycine-rich sequences occurring exclusively in one or both of the non-α-helical terminal domains (21, 48).

DISCUSSION

Several lines of evidence establish the presence of IF in *Helix* esophageal epithelium: (*a*) Single cell preparations revealed a striking pattern of fibrillar bundles in immunofluorescence microscopy. The displays observed (Fig. 4*A*) were very similar to those reported for mammalian intestinal epithelial cells (12, 13), which also form a simple one-layered epithelium. (*b*) *Helix* esophageal cells displayed in electron micrographs typical tonofilament-like bundles. Individual filaments, where resolved, had a diameter of 7–8 nm. Our initial attempts using standard fixation procedures provided a very dense cytoplasm in which filaments were hard to discern. However, a short Triton extraction on previously briefly fixed material (2% formaldehyde for 2 min at 20°C) led to specimens in which the filament display was easily recognized (see below). Material processed in a similar manner could be used for immunoelectron microscopy with a gold-labeled second antibody. Although labeling was sparse, a specific decoration of tono-filament bundles and of individual filaments was easily documented. (*c*) Single cell preparations could be more extensively extracted. Such material was subjected to electron microscopy using negative staining. A dense meshwork of long curvilinear filaments of an approximate diameter of 7–8 nm was seen. These were indistinguishable in morphology from the many previously reported preparations of various mammalian IFs. (*d*) IFs purified on a preparative scale revealed in one-dimensional gel electrophoresis three major polypeptides of 66, 53, and 52 kD, all of which were decorated by the IFA antibody on immunoblots. (*e*) We have used such material after solubilization in 8.5 M urea to reconstitute filaments in vitro. Dialysis against several different buffers (see Results) resulted in filament assembly as seen by negative staining. Such reconstituted filaments revealed in gel electrophoresis the same three major proteins present in the original filament preparation. In conclusion, we have verified by various criteria the presence of non-neuronal IF first indicated by immunofluorescence microscopy of *Helix* epithelia.

Two-dimensional gels on IF purified from the esophagus of *Helix* show that the three major polypeptides of 66, 53, and 52 kD each give rise to several isoforms as do many mammalian IF proteins and particularly the keratins (for references see 34). It is generally assumed that such isoforms reflect different stages of phosphorylation, although we have not proven this point for the *Helix* proteins. Using the internal standards suggested by others and concentrating on the least acidic isoform, the three species have the gel coordinates 66/6.35, 53/6.05, and 52/5.95. Two arguments allow us to suggest that the three polypeptides might be more closely related to mammalian keratins than to other mammalian IF proteins: (*a*) IF display seen in good electron micrographs of mammalian epidermis as well as interior epithelia always emphasized a much tighter packing and bundling of keratin filaments versus IF in nonepithelial cells. The same feature is now documented for the esophageal epithelium of *Helix* where distinct bundles of "tonofilaments" are easily discerned once appropriate extraction and fixation conditions are used. Thus, in line with the keratin expression in epithelia documented so extensively for mammals and particularly man, we hypothesize that the epithelia of *Helix* display keratin-like IF. (*b*) Mammalian keratins differ from all mammalian nonepithelial IF proteins in that they are obligatory heteropolymers both in vivo and in vitro. Recombinant cDNA probes (28), certain immunological cross-reactivities (6), comparative sequence data (21), and two-dimensional gel patterns (34) all suggest that the 20 distinct human keratins are variations on two different prototypes. Corresponding keratin pairs seem to be necessary to provide polymerization-competent protofilament units. This information seems already revealed in most two-dimensional gels (34) that separate the mammalian keratins into two subfamilies: the usually larger and more basic ones versus the generally smaller and more acidic ones. This seems to hold also for the IF proteins purified from *Helix* esophagus. The two smaller polypeptides (53 and 52 kD) are more acidic than are the larger species (66 kD). Densitometric tracings performed on one-dimensional gels provide a molar ratio close to 1 as expected if pairs of 66 plus 53 and 66 plus 52 were to occur.This relatively small complexity of IF proteins in *Helix* esophagus is reminiscent of the situation in human intestine in which only one basic and two acidic keratins are found (34). Nevertheless, there is very little relation between the gel coordinates of the putative *Helix* keratins and the keratins from either human intestine or esophagus. Final proof for the keratin nature of the IFs from *Helix* esophagus will have to await either reconstitution experiments on the separated polypeptides and their mixtures, or amino

acid sequence data. Nevertheless, we can note that the filament reconstitution conditions of 2–50 mM Tris buffer found for the *Helix* proteins resemble those of mammalian keratins rather than those of mammalian nonepithelial IF proteins that require the addition of salt (see for instance reference 25).

Given the results on *Helix* IFs, how should one interpret negative results with anti-IFA on some other invertebrates? Before concluding that there is an absence of IF, some particular properties of the anti-IFA must be considered. Anti-IFA was originally raised against human glial fibrillary acidic protein and was shown to detect all five IF classes in mammals (44). Subsequent studies located the epitope towards the carboxyterminal part of the α-helical middle domain into a region which by sequence is highly homologous in all IF proteins including the wool α-keratins (18, 52). However, recent results with anti-IFA on human keratins using immunoblotting show that some keratins, mainly the smaller and acidic ones, react with noticeably lower affinity than do others (6). Because of this weak affinity, ascites fluids were used at relatively low dilution, and we have also used a similar concentration in our immunoblotting experiments, i.e., ~60 μg/ml. The most likely interpretation of these results on anti-IFA is that relatively subtle amino acid exchanges in the IFA epitope can strongly influence the reactivity of different IF proteins. Just as some human keratins have only weak affinity in comparison with others, it remains possible that some IF proteins in more distant species are not detected at all by anti-IFA. A further complication with the antibody at least in immunofluorescence microscopy concerns the fixation procedures. It has been our experience that the simplest fixation, i.e., the use of −10°C methanol or acetone so often used to document vertebrate IFs by other antibodies, resulted in poor or negligible staining of cultured mammalian cells when anti-IFA hybridoma supernatants were used. Strongly improved reactions were seen with 5% acetic acid in ethanol but such treatment is not suitable for subsequent immunoelectron microscopy. Good and convincing staining was observed on cells and tissues subjected to a short fixation with 2% formalin and then treated with Triton. It is, however, important that the formalin fixation is very brief (2 min at 20°C). Prolonged fixation led again to poor reactivity either because of too strong cross-linking or the presence of an aldehyde-reactive amino acid side chain within the epitope. Further increase in antibody concentration is not suggested as we have already used the monoclonal IgGs at ~130 μg/ml, a value much higher than is usually necessary for good monoclonal or affinity-purified polyclonal antibodies. We therefore conclude that anti-IFA is a valuable marker for IF if a positive immunofluorescence reaction is observed under optimal conditions. However, lack of staining by anti-IFA particularly on invertebrate tissues seems insufficient to conclude that there is an absence of IFs.

In our limited survey of invertebrates (Table I), we have found positive staining of epithelia by anti-IFA for *Lumbricus*, *Arenicola*, and *Ascaris*. In view of our results on *Helix* esophagus, we consider this staining a good guide for the possible presence of non-neuronal IF. However, until the reactivity of this antibody on invertebrate tissues is better understood, experiments on the biochemical and electron microscopic level have to be done to prove the existence of IF. For instance, we cannot explain why we failed to detect decoration with anti-IFA on *Drosophila* tissues even though cultured *Drosophila* cells contain an insoluble 46-kD protein that seems to be recognized by this antibody in immunoblotting (51). This protein is thought to be an IF protein because it cross-reacts with mammalian vimentin as seen with a further monoclonal antibody (9, 51). Although one could argue that the negative hybridization data with mammalian vimentin and desmin DNA probes on *Drosophila* (46) may be due to a high degree of sequence variation of the putative vimentin-related protein(s) of the insect, one can still not rule out that the immunological cross-reactivity is purely fortuitous, as convincing ultrastructural evidence for IF has not been provided. A further difficulty concerns *Tetrahymena* where a 49-kD protein assembles into filaments with a diameter of 14 nm (37, 38). Although we were unable to stain *Tetrahymena* with anti-IFA, this is insufficient to argue that IFs are not present. Indeed the main problem concerning IFs in this ciliate lies in the ultrastructural appearance of the 14-nm filaments, which are built from globular units (37). IF structure, however, is known to arise from rod-like elements due to the presence of α-helices in coiled-coil conformation (16, 17, 48, 52).

In spite of these difficulties, we feel that IF are more widespread through invertebrates than is currently thought. We have assembled for the first time strong ultrastructural as well as biochemical evidence for the existence of non-neuronal IF in epithelia of the mollusc *Helix pomatia*. These data complement existing evidence on invertebrate neurofilaments. In molluscs, the polypeptide molecular weights are 60 and 200 kD for *Loligo* (31, 43, 54), and 60 and 65 kD for *Aplysia* (32). In addition, *Myxicola*, an annelid, is known to have neurofilament proteins of 150 and 160 kD (8, 20, 31, 43). Although it is generally thought that arthropods lack neurofilaments (32, 51), the situation is not very clear given the presence of paired helical filaments in the giant neurones of the whip spider *Heterophrynus longicornis* (10). These structures are highly reminiscent of the filament tangles found in humans suffering from Alzheimer's disease (53). Here they are thought to be derived from neurofilaments (1), although a molecular proof of this hypothesis is lacking. Using the occasional electron micrographs as a starting point, one is encouraged to search for the possible IF nature of various membrane-attached filaments reported for certain invertebrate cell types (2, 5, 22, 26, 45). As IFs seem absent in a few vertebrate cells (24, 42, 50), it may not be too surprising if some invertebrate species also lack this filament type. However, to understand IF divergence on an evolutionary scale requires a better analysis of invertebrate IF proteins. Towards this aim two experimental approaches are now indicated: (*a*) to explore the possibility using biochemical procedures and electron microscopy that a typical epithelium of an invertebrate not stained by anti-IFA could nevertheless contain IF. Here the use of the extraction–fixation procedures developed for *Helix* esophagus may be helpful, and (*b*) to use biochemical and immunological procedures to assess if different IF proteins are expressed in different cell types of the same invertebrate, and to see whether the rules of cell type–specific expression are the same or different from those established for vertebrates.

We thank Dr. Martin Raff for the anti-IFA hybridoma, S. Fischer for help with the amino acid composition, and H.-G. Tölle for discussion.

E. Bartnik is at the Fachbereich für Biologie at the University of Bonn and is supported by a predoctoral fellowship from the Max Planck Society.

Received for publication 11 February 1985, and in revised form 3 April 1985.

Note Added in Proof: Well-preserved IFs are also documented electron microscopically in glia cells of the annelid *Aphrodite aculeata* (see Figs. 89 and 460 in Fawcett, O. W., 1981, The Cell, W. B. Saunders Co., Philadelphia), and we have characterized such displays also in glia cells of molluscs, including *Helix pomatia* (manuscript in preparation).

REFERENCES

1. Anderton, B. H., D. Breinburg, M. J. Downes, P. J. Green, B. E. Tomlinson, J. Ulrich, J. N. Wood, and J. Kahn. 1982. Monoclonal antibodies show that neurofibrillary tangles and neurofilaments share antigenic determinants. *Nature.* 298:84–86.
2. Bilbant, A. 1980. Cell junctions in the excitable epithelium of bioluminiescent scales on a polynoid worm: a freeze-fracture and electrophysiological study. *J. Cell Sci.* 41:341–368.
3. Burton, P. R., and R. E. Hinkley. 1974. Further electron microscopic characterization of axoplasmic microtubules of the ventral nerve cord of the crayfish. *J. Submicrosc. Cytol.* 6:311–326.
4. Bretscher, A., and K. Weber. 1978. Localization of actin and microfilament-associated proteins in the microvilli and terminal web of the intestinal brush border by immunofluorescence microscopy. *J. Cell Biol.* 79:839–845.
5. Coggeshall, R. E. 1967. A light and electron microscope study of the abdominal ganglion of *Aplysia californica*. *J. Neurophysiol.* 30:1263–1287.
6. Cooper, D., A. Schermer, R. Pruss, and T. T. Sun. 1984. The use of aIF, AE1 and AE3 monoclonal antibodies for the identification and classification of mammalian epithelial keratins. *Differentiation.* 28:30–35.
7. Debus, E., K. Weber, and M. Osborn. 1982. Monoclonal cytokeratin antibodies that distinguish simple from stratified squamous epithelia: characterization on human tissues. *EMBO (Eur. Mol. Biol. Organ.) J.* 1:1641–1647.
8. Eagles, P. A. M., D. S. Gilbert, and A. Meggs. 1981. The polypeptide composition of axoplasm and neurofilaments from the marine worm *Myxicola infundibulum*. *Biochem. J.* 199:89–100.
9. Falkner, F. G., H. Saumweber, and H. Biessmann. 1981. Two *Drosophila melanogaster* proteins related to intermediate filament proteins of vertebrate cells. *J. Cell Biol.* 91:175–183.
10. Foelix, R. F., and M. Hauser. 1979. Helically twisted filaments in giant neurons of a whip spider. *Eur. J. Cell Biol.* 19:303–306.
11. Franke, W. W., E. Schmid, S. Winter, M. Osborn, and K. Weber. 1979. Widespread occurrence of intermediate-sized filaments of the vimentin-type in cultured cells from diverse vertebrates. *Exp. Cell Res.* 123:25–46.
12. Franke, W. W., B. Appelhans, E. Schmid, C. Freudenstein, M. Osborn, and K. Weber. 1979. The organization of cytokeratin filaments in the intestinal epithelium. *Eur. J. Cell Biol.* 19:255–268.
13. Franke, W. W., S. Winter, C. Grund, E. Schmid, D. L. Schiller, and E. D. Jarasch. 1981. Isolation and characterization of desmosome-associated tonofilaments from rat intestinal brush border. *J. Cell Biol.* 90:116–126.
14. Franke, W. W., E. Schmid, D. L. Schiller, S. Winter, E. D. Jarasch, R. Moll, H. Denk, B. W. Jackson, and K. Illmensee. 1982. Differentiation-related patterns of expression of proteins of intermediate-size filaments in tissues and cultured cells. *Cold Spring Harbor Symp. Quant. Biol.* 46:431–453.
15. Fuchs, E., and H. Green. 1978. The expression of keratin genes in epidermis and cultured epidermal cells. *Cell.* 15:887–897.
16. Fuchs, E., and D. Marchuk. 1983. Type I and type II keratins have evolved from lower eukaryotes to form the epidermal intermediate filaments in mammalian skin. *Proc. Natl. Acad. Sci. USA.* 80:5857–5861.
17. Geisler, N., E. Kaufmann, and K. Weber. 1982. Protein chemical characterization of three structurally distinct domains along the protofilament unit of desmin 10 nm filaments. *Cell.* 30:277–286.
18. Geisler, N., E. Kaufmann, S. Fischer, U. Plessmann, and K. Weber. 1983. Neurofilament architecture combines structural principles of intermediate filaments with carboxy-terminal extensions increasing in size between triplet proteins. *EMBO (Eur. Mol. Biol. Organ.) J.* 2:1295–1302.
19. Gigi, O., B. Geiger, Z. Eshhar, R. Moll, E. Schmid, S. Winter, D. L. Schiller, and W. W. Franke. 1982. Detection of a cytokeratin determinant common to diverse epithelial cells by a broadly cross reacting monoclonal antibody. *EMBO (Eur. Mol. Biol. Organ.) J.* 1:1429–1437.
20. Gilbert, D. S. 1975. Axoplasm architecture and physical properties as seen in the *Myxicola* giant axon. *J. Physiol. (Lond.).* 253:257–301.
21. Hanukoglu, I., and E. Fuchs. 1983. The cDNA sequence of a type II cytoskeletal keratin reveals constant and variable structural domains among keratins. *Cell.* 33:915–924.
22. Harris, P., and G. Shaw. 1984. Intermediate filaments, microtubules and microfilaments in epidermis of sea urchin tube foot. *Cell Tissue Res.* 236:27–33.
23. Holtzer, H., G. S. Bennett, S. J. Tapscott, J. M. Croop, and Y. Toyama. 182. Intermediate-size filaments: changes in synthesis and distribution of the myogenic and neurogenic lineage. *Cold Spring Harbor Symp. Quant. Biol.* 46:317–329.
24. Jackson, B. W., C. Grund, E. Schmid, K. Bürki, W. W. Franke, and K. Illmensee. 1980. Formation of cytoskeletal elements during mouse embryogenesis. Intermediate filaments of the cytokeratin type and desmosomes in preimplantation embryos. *Differentiation.* 17:161–179.
25. Jorcano, J. L., M. Rieger, J. K. Franz, D. L. Schiller, R. Moll, and W. W. Franke. 1984. Identification of two types of keratin polypeptides within the acidic cytokeratin subfamily I. *J. Mol. Biol.* 179:257–281.
26. Kensler, R. W., P. R. Brink, and M. M. Dewey. 1979. The septum of the lateral axon of the earthworm: a thin section and freeze fracture study. *J. Neurocytol.* 8:565–590.
27. Kilmartin, J. V., B. Wright, and C. Milstein. 1982. Rat monoclonal antibodies derived by using a new nonsecreting rat cell line. *J. Cell Biol.* 93:576–582.
28. Kim, K. H., J. Rheinwald, and E. V. Fuchs. 1983. Tissue specificity of epithelial keratins: differential expression of mRNAs from two multigene families. *Mol. Cell. Biol.* 3:495–502.
29. Kniprath, E. 1970. Die Feinstruktur der Periostrakumgrube von *Lymnaea stagnalis*. *Biomineralisation.* 2:23–37.
30. Laemmli, U. K. 1970. Cleavage of structural proteins during the assembly of the head of bacteriophage T4. *Nature (Lond.).* 227:680–685.
31. Lasek, R. J., N. Krishnan, and J. R. Kaiserman-Abramof. 1979. Identification of the subunit proteins of 10-nm neurofilaments isolated from axoplasma of squid and *Myxicola* giant axons. *J. Cell Biol.* 82:336–346.
32. Lasek, R. J., M. M. Oblinger, and P. F. Drake. 1983. Molecular biology of neuronal geometry: expression of neurofilament genes influences axonal diameter. *Cold Spring Harbor Symp. Quant. Biol.* 48:731–744.
33. Lazarides, E. 1980. Intermediate filaments as mechanical integrators of cellular space. *Nature (Lond.).* 283:249–256.
34. Moll, R., W. W. Franke, D. L. Schiller, B. Geiger, and R. Krepler. 1982. The catalog of human cytokeratins: patterns of expression in normal epithelia, tumors and cultured cells. *Cell.* 31:11–24.
35. Nadelhaft, J. 1974. Microtubule densities and total numbers in selected axons of the crayfish abdominal nerve cord. *J. Neurocytol.* 3:73–86.
36. Neukirchen, R. O., B. Schlosshauer, S. Baars, H. Jäckle, and U. Schwang. 1982. Two-dimensional protein analysis at high resolution on a microscale. *J. Biol. Chem.* 257:15229–15234.
37. Numata, O., and Y. Watanabe. 1982. *In vitro* assembly and disassembly of 14-nm filament from *Tetrahymena pyriformis*. The protein component of 14-nm filament is a 49,000-dalton protein. *J. Biochem. (Tokyo).* 91:1563–1573.
38. Numata, O., T. Sugai, and Y. Watanabe. 1985. Control of germ cell nuclear behaviour at fertilization by *Tetrahymena* intermediate filament protein. *Nature (Lond.).* 314:192–194.
39. O'Farrell, P. H. 1975. High resolution two-dimensional electrophoresis of proteins. *J. Biol. Chem.* 250:4007–4021.
40. Olsson, R. 1961. The skin of amphioxus. *Zeitschr. f. Zellforsch.* 54:90–104.
41. Osborn, M., N. Geisler, G. Shaw, G. Sharp, and K. Weber. 1982. Intermediate filaments. *Cold Spring Harbor Symp. Quant. Biol.* 46:413–429.
42. Paulin, D., C. Babinet, K. Weber, and M. Osborn. 1980. Antibodies as probes of cellular differentiation and cytoskeletal organization in the mouse blastocyst. *Exp. Cell Res.* 130:297–304.
43. Phillips, L. L., L. Autilio-Gambetti, and R. J. Lasek. 1983. Bodian's silver method reveals molecular variation in the evolution of neurofilament proteins. *Brain Res.* 278:219–223.
44. Pruss, R. M., R. Mirsky, M. C. Raff, R. Thorpe, A. J. Dowding, and B. H. Anderton. 1981. All classes of intermediate filaments share a common antigenic determinant defined by a monoclonal antibody. *Cell.* 27:419–428.
45. Pumplin, D. W., and K. J. Muller. 1983. Distinctions between gap junctions and sites of intermediate filament attachment in the leech C.N.S. *J. Neurocytol.* 12:805–815.
46. Quax, W., R. Van Den Heuvel, W. V. Egberts, Y. Quax-Jeuken, and H. Bloemendal. 1984. Intermediate filament cDNAs from BHK21 cells: demonstration of distinct genes for desmin and vimentin in all vertebrate classes. *Proc. Natl. Acad. Sci. USA.* 81:5970–5974.
47. Runham, N. W. 1975. Alimentary canal. *In* Pulmonates. Volume 1. Functional Anatomy and Physiology V. Fretter and J. Peake, editors. Academic Press, Inc., London/New York/San Francisco. 53–104.
48. Steinert, P. M., R. H. Rice, D. R. Roop, B. L. Trus, and A. C. Steven. 1983. Complete amino acid sequence of a mouse epidermal keratin subunit and implications for the structure of intermediate filaments. *Nature (Lond.).* 302:794–800.
49. Towbin, H., T. Staehelin, and J. Gordon. 1979. Electrophoretic transfer of proteins from polyacrylamide gels to nitrocellulose sheets: procedure and some applications. *Proc. Natl. Acad. Sci. USA.* 76:4350–4354.
50. Venetianer, A., D. L. Schiller, T. Magin, and W. W. Franke. 1983. Cessation of cytokeratin expression in a rat hepatoma cell line lacking differentiated functions. *Nature (Lond.).* 305:730–733.
51. Walter, M. F., and H. Biessmann. 1984. Intermediate-sized filaments in *Drosophila* tissue culture cells. *J. Cell Biol.* 99:1468–1477.
52. Weber, K., G. Shaw, M. Osborn, E. Debus, and N. Geisler. 1983. Neurofilaments, a subclass of intermediate filaments: structure and expression. *Cold Spring Harbor Symp. Quant. Biol.* 47:717–729.
53. Wisniewski, H. M., H. K. Narang, and R. D. Terry. 1976. Neurofibrillary tangles of paired helical filaments. *J. Neurol. Sci.* 27:173–181.
54. Zackroff, R. V., and R. D. Goldman. 1980. *In vitro* reassembly of squid brain intermediate filaments (neurofilaments): purification by assembly-disassembly. *Science (Wash. DC).* 208:1152–1155.